PROCEEDINGS OF SCIENCE

Medical Image Segmentation based on Improved Fuzzy Clustering in Robot Virtual Surgical System

Yidong Bao

State Key Laboratory of Robotics and System, Harbin Institute of Technology, Harbin 150080, P.R. China.

School of Software, Pingdingshan University, Pingdingshan 467000, P.R. China.

Email: baoyidong2012@163.com

Dongmei Wu

State Key Laboratory of Robotics and System, Harbin Institute of Technology, Harbin 150080, P.R. China.

Email: wudmhit@163.com

In view of the problems relating to the precision and convergence rate of traditional ant colony algorithm and fuzzy clustering algorithm on the medical image segmentation, a modified self-adaptive threshold ant colony optimization and fuzzy clustering (SAAF) algorithm were proposed here to realize the segmentation of the complex background medical image. As to the complex medical image, Otsu algorithm was firstly performed to obtain the optimal threshold, the local optimal solution of ant colony algorithm was avoided through the intervention of optimal threshold, then the clustering center and the number of cluster classes obtained through the self-adaptive threshold ant colony algorithm were imported into the fuzzy clustering algorithm until the image segmentation was finalized. The doctor can get the diseased organ by SAAF image segmentation algorithm according to the CT scanned images, and can use the segmented organ image to build the 3D virtual organ tissue model. Then, the doctor can achieve virtual surgical before using the real robot surgical to operate on patients. It will greatly improve the success rate of surgery and efficiency.

ISCC 2015
18-19, December, 2015
Guangzhou, China

PoS(ISCC2015)040

1. Introduction

Using the surgical robot to operate on patients is the latest operation option. The surgical operation by the surgical robot has the characteristics of high precision, small incision and long-time operation. Thus, the surgical operation by the surgical robot is the latest research focus and hotspot. However, any doctor must receive the repeated training and be skillful at the surgical operation by robot. The surgical training by medical staff will be troubled by a lot of inconvenience due to the limitation of traditional surgical training mode using corpse or animal [1]. Therefore, a new alternative is offered for doctors to receive the training of surgical robot using the virtual surgical training system developed by the computer technology. In the virtual surgical training system, the establishment of an effective soft tissues model is the key to the entire system. With a view to the establishment of the soft tissues organ model, the clear 2D image contour should be obtained to the extent possible through image processing according to the medical image of the patient's organs. Then the 3D virtual soft tissues model was built according to the 2D image of organs, and was loaded to the virtual training system. Ultimately the force feedback force was manipulated to finalize the training of virtual surgery. Thus, the processing of the medical image of the patient's organs is the key to building effective virtual soft tissues. The medical image segmentation technique is one of the key technologies for medical image processing. According to different imaging principles, the medical image can be divided into a many different models, such as ultrasound, nuclear magnetic resonance imaging, single-photon emission computed tomography, positron emission tomography and computed tomography [2]. Compared to other imaging methods, CT has higher density resolution, and CT has a significant presence in the clinical diagnosis for organ tumor [3]. For this reason, the processing and segmentation of CT medical image is focally examined here.

Through the preliminary analysis and research, the fuzzy clustering and ant colony algorithm were performed here to segment the medical image. The fuzzy clustering algorithm (FCM) is the process of image segmentation through the unsupervised fuzzy class calibration method. However, some deficiencies are also found in FCM: on the one hand, the number of clustering classes should be firstly set, which results in the lowered precision in image segmentation; on the other hand, the uncertainty of setting the clustering classes leads to the large amount of calculation and a lot of time in the clustering process, decreasing the efficiency. Balafar proposed a new clustering method which can select training data for each target class based on FCM for medical segmentation[4]. Biniaz presented an Unsupervised ACO developed by FCM which utilizes the benefits of two algorithms and overlaps their defects, and this method is less sensitive to noise[5]. Zhang used a hybrid roughness-based FCM mathematic model for medical image segmentation[6]. Chen proposed a local fuzzy clustering and Chan-Vese model for CT medical image segmentation[7]. This model can efficiently reduce the time complexity. Zhang compared the different algorithms for medical image segmentation method, and pointed out the further research direction of this method[8].

In addition to using FCM method, there are other common methods for the image segmentation based on different threshold methods. For example, LAN proposed an optimized interactive image segmentation algorithm which can improve the segmentation accuracy[9]. Sofian presented an automated segmentation method which was to use Otsu thresholding in segmenting and detecting the outer boundary[10]. Manikandan proposed a segmentation algorithm of medical brain images[11]. This method is real coded genetic algorithm with Simulated Binary Crossover based on multilevel thresholding.

To improve the FCM algorithm clustering center and the number of clustering classes calibration method, overcome the traditional ant colony algorithm which may easily fall into the local optimal problem, and further increase the convergence rate, the ant colony algorithm using the self-adaptive threshold was proposed here, which combined FCM and Otsu threshold methods to segment the medical image. The modified Otsu algorithm was firstly performed to obtain the optimal threshold, the ant colony algorithm falling into the local optimal solution was avoided through the intervention of the optimal threshold, the clustering center and the number

of clustering classes those were further obtained from the self-adaptive threshold ant colony algorithm were imported into FCM, until the medical image was segmented. Comparing the image segmentation method using Traditional ant colony algorithm (TA), Ant fuzzy colony clustering algorithm (AF) and quantum ant colony fuzzy clustering algorithm (QAF), the experimental verification figure and data demonstrate that the algorithm has been greatly improved in terms of time and the misclassification error.

2. Self-Adaptive Threshold Ant Colony Fuzzy Clustering Algorithm

The image processing procedure of SAAF is given below:

(1) The image preprocessing was firstly done to read the image, which was later converted to the double-precision grey-scale image.

(2) The image underwent the Otsu self-adaptive threshold segmentation was to obtain the optimal value T .

The grey level of the original image was assumed as V and the grey level range of the image was set as $\{0,1,\cdots V-1\}$. The number of pixels at the grey level of i was assumed as n_i, the total number of pixels obtained is $N=\sum_{i=0}^{V-1} n_i$, and the probability for the emergence of each grey value is $P_i=\frac{n_i}{N}$. The grey level q was set as the boundary and the image was classified into the target region and background region. The regions when the grey level is $1\sim q$, $q+1\sim V-1$ was set as the background region A and B respectively.

The probability of A and B can be wrote as

$$P_B=\sum_{i=q+1}^{V-1} P_i \tag{2.1}$$

The gray average of A and B can be wrote as

$$\wp_A=\frac{\sum_{i=0}^{q} i\cdot P_i}{P_A} \tag{2.2}$$

$$\wp_B=\frac{\sum_{i=q+1}^{V-1} i\cdot P_i}{P_B} \tag{2.3}$$

Then, the sum of gray average is

$$\wp=\sum_{i=0}^{V-1} i\cdot P_i \tag{2.4}$$

The class variance between Target Area and background area can be wrote as

$$\delta^2=P_A(\varphi_A-\varphi)^2+P_B(\varphi_B-\varphi)^2 \tag{2.5}$$

E was made the optimal eigenvalue when δ^2 was the biggest, it can be wrote as

$$E=Arg_{\max}[P_A(\varphi_A-\varphi)^2+P_B(\varphi_B-\varphi)^2] \tag{2.6}$$

(3) Each pixel Y_i of the original image was seen as an ant, while the ant matrix and each parametric variable were initialized, the clustering radius, the volatilization rate and the initialization offset error were set as $r=90$, $Rho=0.95$ and $\wp_0$ respectively; the image matrixes were initialized and the clustering center was supervised; and the number of iterations was set as M .

(4) Here, we supposed that the pheromone of each path is zero in initial. Using the equation

$$\Im_{ik}(t)=\begin{Bmatrix}1\\0\end{Bmatrix}\quad\begin{matrix}D_{ij}\leqslant r\\D_{ij}>r\end{matrix} \tag{2.7}$$

The residual pheromone left by ants on the path was calculated, in which D_{ij} is the Euclidean distance between the pixel Y_i and Y_j .

(5) As the optimization process cycles, each path residues and subsequent change of information, and the residual information content left on each path will also change.

$$\Im_{ij}(t+1)=rho\cdot\Im_{ij}(t)+\frac{W}{D_{ij}} \tag{2.8}$$

W is information intensity. Using the equation

$$P_{ij}(t)=\frac{\Im_{ij}^{o}(t)(\frac{1}{D_{ij}(t)})^{\lambda}}{\sum_{g=1}^{j}\Im_{ig}^{o}(t)(\frac{1}{D_{ig}(t)})^{\lambda}} \tag{2.9}$$

The selection probability of ant colony for the path was obtained, in which o and λ are the influencing factors. $P_{ij}(t)$ was compared with the optimal eigenvalue E obtained from Step one, if $P_{ij}(t)>E$, then Y_i is classified into the Y_j neighborhood, otherwise Y_i is marked as unclassified and will be further classified. We set $I_k=\{D_{ig}\leqslant r, i=1,2,\cdots,w\}$, in which I_k is the set classified into the Y_i neighborhood. Then, the optimal cluster center can be wrote as

$$T_j=\frac{1}{u}\sum_{i=1}^{u}Y_i, Y_j\in I_j \tag{2.10}$$

The cluster offset error of j is

$$G_j=\sum_{g=1}^{j}[\sum_{i=1}^{z}(y_{gi}-T_{ji})^2]^{1/2} \tag{2.11}$$

The sum of offset error can be calculated according to Eq. (15). It is $\wp=\sum_{j=1}^{g}G_j$. If $\wp\leqslant\wp_0$, output the number of optimal cluster m and cluster center $Q_i(i=1,2\cdots m)$.

(6) The clustering center of the fuzzy clustering algorithm was initialized by using the clustering center Q_i obtained from the self-adaptive ant colony algorithm, the number of clusters m was used as the number of classes of the fuzzy clustering, and the membership matrix was initialized.

(7) Computer membership

$$\underset{\tilde{ij}}{R}=[\sum_{g=1}^{m}\left(\frac{d_{ij}(m_j,\hbar_i)^{\frac{2}{b-1}}}{d_{gj}(y_j,\hbar_j)}\right)^{-1}] \tag{2.12}$$

b is weighted index. The value of b is 2. Updating cluster center, and computer objective function

$$H(R,Q)=\sum_{j=1}^{n}\sum_{i=1}^{m}(R_{ij})^{b}d_{ij}^{2}(Y_{j},Q_{i}) \tag{2.13}$$

(8) The distance between the updated clustering center and the clustering center acquired from the last step was calculated, and the image will be output if the distance is within the defined error range.

Fig. 1 is the flow chart of SAAF algorithm.

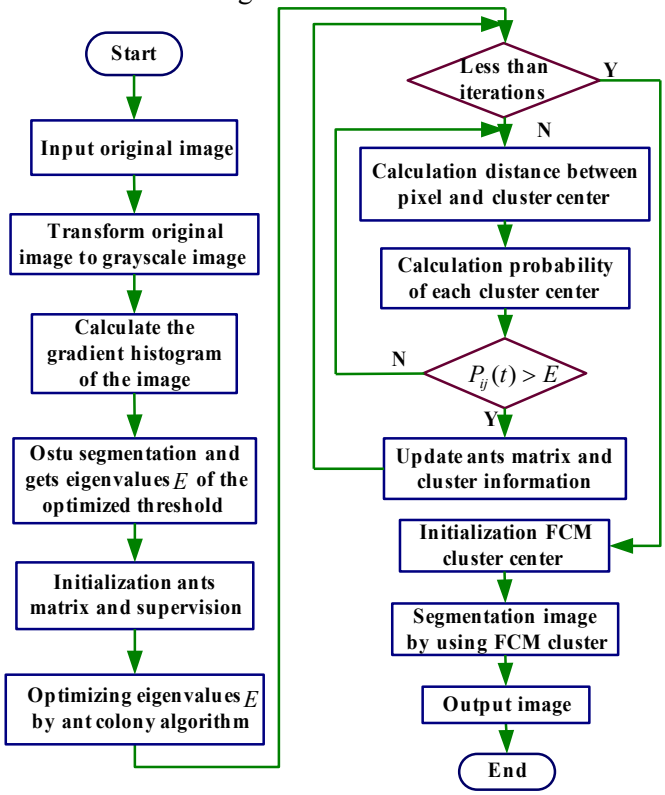

Figure 1: The Flow Chart of SAAF Algorithm

3. Experiment Results

To verify the correctness and effectiveness of the modified algorithm, the experiment verification figure and relevant data were obtained by comparing the image segmentation methods using AF, QAF [12], and SAAF, so as to compare and demonstrate the effectiveness of this modified algorithm.

Fig. 2(a), Fig. 3(a) and Fig. 4(a) are the original organ CT images. Fig. 2(b) and Fig. 3(b) are the segmented figures using AF algorithm. Fig. 4(b) is the segmented figure using QAF. Fig. 2(c), Fig. 3(c) and Fig. 4(c) are the segmented figures using SAAF algorithm. The experiment verification figure clearly suggests that the image segmented which uses SAAF algorithm is clearer, particularly of the image edge, than the segmented contour described in AF and QAF [12].

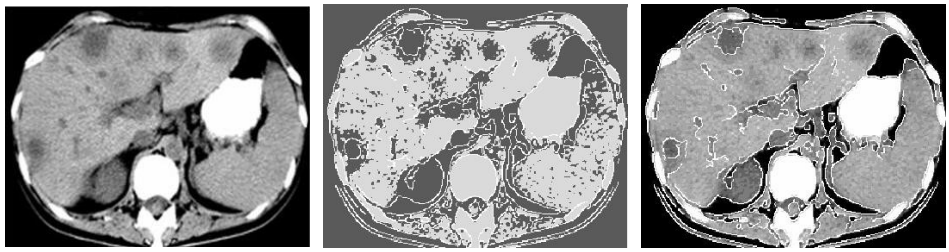

Figure 2: (a) Liver image (b) AF segmentation results (c) SAAF segmentation results

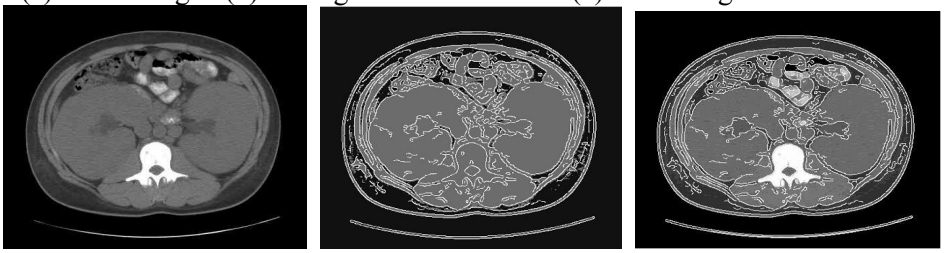

Figure 3: (a) Kidney image (b) AF segmentation results (c) SAAF segmentation results

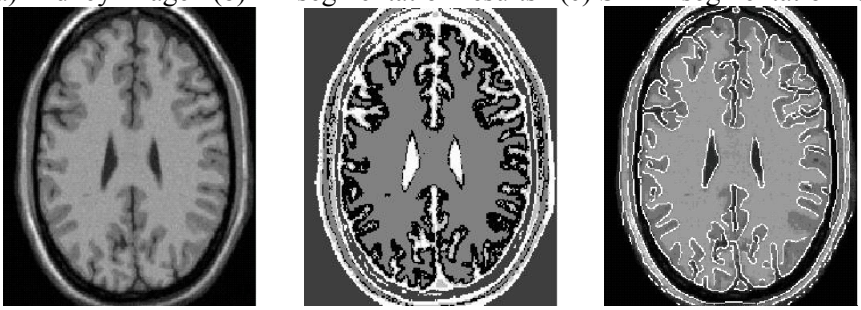

Figure 4: (a) Brain image (b) QAF segmentation results [12] (c) SAAF segmentation results

In the experiment, the average times for calculating the distance between the clustering center after 15 updates and the clustering center previously obtained were recorded, as shown in Table 1. This discovers that the calculation times using SAAF were less than those using TA and AF. Table 2 presents the thresholds running three different methods, which indicates that the ultimate threshold obtained from SAAF is a different self-adaptive value, and is optimal than the first two methods. During the process of experiment, given the same number of iterations, the number of iterations was selected as 100, 200 and 300 times here, the average value was obtained after running 30 times, and the time spent in TA, AF and SAAF is shown in Table 3. And given the same number of iterations, the time spent in SAAF is less than that in the first two methods. Table 4 means the error classification and kappa coefficient as to the image segmented using different methods compared with the original image, which indicates that the error classification for SAAF is less than that for AF, and kappa coefficient is higher for SAAF than that for AF.

	Numbers of calculation distance	
	AF (Count)	SAAF(Count)
Fig. 2	8	6
Fig. 3	7	4
Fig. 4	9	7

Table 2: Number of Calculation Distance of Different Algorithms

	Numbers of iteration	Time (s)		
		TA	AF	SAAF
Fig. 2	100	18.32	22.67	11.32
	200	27.87	31.95	20.21
	300	35.12	39.54	26.17
Fig. 3	100	22.32	26.78	12.13
	200	28.15	30.45	25.65
	300	38.47	40.32	30.81
Fig. 4	100	11.32	19.56	8.27
	200	18.96	26.73	13.33
	300	29.42	34.87	19.55

Table 2: Spend Time of Different Algorithms and Iteration

	Threshold		
	TA	AF	SAAF
Fig. 2	0.75	0.75	0.4421
Fig. 3	0.78	0.78	0.4529
Fig. 4	0.67	0.67	0.3657

Table 3: Threshold of Different Algorithms

	Classification error rate		Kappa coefficient	
	AF	SAAF	AF	SAAF
Fig. 2	5.11%	3.17%	0.946	0.969
Fig. 3	5.59%	3.32%	0.922	0.962
Fig. 4	4.78%	2.86%	0.957	0.972

Table 4: The Classification Error Rate and Kappa Coefficient

4. Applying Saaf Into Robot Virtual Surgical System

With diseased liver, for example, the liver that needs to be operated will be separated from the whole CT image after the SAAF segmentation. And using the position precision and separation algorithm, we will partition the image into separate liver image according to the liver outline. Then, the 3D virtual liver tissue model would be established according to the size and the location of the diseased liver. This virtual liver tissue model has the characteristic of viscoelasticity, also it has the same diseased location and character with the real liver organ. Then, the 3D virtual liver tissue model would be loaded into the robot virtual surgical training system. Using haptic force-feedback device to achieve cutting simulation and other operation for the diseased liver. Fig. 5 shows the 3D virtual liver tissue model which established by VC++ and OpenGL according to SAAF image segmentation algorithm. It can achieve virtual liver squashes and cutting simulation.

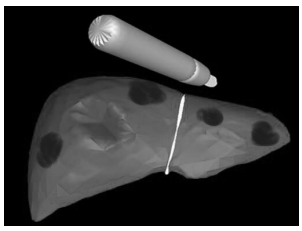

Figure 5: The 3D virtual liver tissue model according to SAAF segmentation

5. Conclusion

In this paper, Otsu algorithm was firstly used to obtain the optimal threshold, the ant colony algorithm falling into the local optimal solution was avoided through the threshold of the optimal threshold, the clustering center and the number of cluster classes further obtained

through the self-adaptive threshold ant colony algorithm were imported to the fuzzy C-mean cluster algorithm, until the image segmentation was finalized. The effect of image segmentation using TA, AF and QAF were experimentally compared, validating SAAF with higher time efficiency; less average times of calculating the distance between the clustering centers; smaller error classification, higher kappa coefficient, and also validating the effectiveness and correctness of SAAF. While this algorithm further improves the segmentation of medical image, when the target and background are very close, the precision needs to be further improved, therefore the subsequent works will further make improvements based on previous efforts.

References

[1] G. Picinbono, H. Delingette, N. Ayache. Non-linear and anisotropic elastic soft tissue models for medical simulation. IEEE International Conference Robotics and Automation.Institute of Electrical and Electronics Engineers Inc Seoul, Korea 2: 1370-1375(2001)

[2] G. Q. Xing，Z. Liu, Y. B. Li. *MATLAB in application of medical image segmentation* . Chinese J Med Imaging. 16(6): 453-455(2008) (In Chinese)

[3] L. Q. Lin, L. L. Chen. *Segmentation for CT images of liver neoplasms based on MATLAB* . Beijing Biomedical Engineering. 31(3): 241-244(2012) (In Chinese)

[4] M. A. Balafar, R. A. B. D. Rahman, M. I. Saripan, S. Mashohor, R. Mahmud. *Medical image segmentation using fuzzy C-mean (FCM) and user specified data* . Journal of Circuits, Systems and Computers. 19(1): 1-14(2010)

[5] A. Biniaz, A. Abbasi. *Unsupervised ACO: Applying FCM as a supervisor for ACO in medical image segmentation*. Journal of Intelligent and Fuzzy Systems. 27(1): 407-417(2014)

[6] B. W. Zhang, S. Y. Qian, B. W. Song. *Application of Improved FCM in Medical Image Segmentation*. Computer Engineering. 38(14): 193-195(2012) (In Chinese)

[7] J. X. Chen, L. N. Chen, L. H. Li. A Local Fuzzy-based Chan-Vese Method for the Segmentation of CT Medical Images. Journal of University of South China (Science and Technology). 29(2): 108-113(2015) (In Chinese)

[8] F. Zhang, H. Fan. *Research on medical image segmentation based on fuzzy C-means clustering algorithm*. Computer Engineering and Applications. 50(4): 144-151(2014) (In Chinese)

[9] H. Lan, L. Min. *Interactive segmentation algorithm optimized by multi-threshold with application in medical images*. Journal of Computer Applications. 33 (5): 1435-1438(2013)

[10] H. Sofian, J.C.M. Than, N. N Mohd, H. Dao. *Segmentation and detection of media adventitia coronary artery boundary in medical imaging intravascular ultrasound using Otsu thresholding* . 2015 International Conference on BioSignal Analysis, Processing and Systems (ICBAPS),IEEE Xplore, Kuala Lumpur, Malaysia, 72-6(2015)

[11] S. Manikandan, K. Ramar, I. M. Willjuice, K. G. Srinivasagan. *Multilevel thresholding for segmentation of medical brain images using real coded genetic algorithm* . Measurement: Journal of the International Measurement Confederation. 47 (1): 558-568(2014)

[12] J. Y. Li, J. W. Dang. *Image segmentation based on quantum ant colony fuzzy clustering algorithm* . Opto-Electronic Engineering. 40(1): 126-131(2013) (In Chinese)